Published in final edited form as:
Nat Med. 2009 September ; 15(9): 1066–1071. doi:10.1038/nm.2007.

Interferon regulatory factor 8 regulates bone metabolism by suppressing osteoclastogenesis

Baohong Zhao[1,2], **Masamichi Takami**[1], **Atsushi Yamada**[1], **Xiaogu Wang**[1], **Takako Koga**[3], **Xiaoyu Hu**[2,4], **Tomohiko Tamura**[5], **Keiko Ozato**[5], **Yongwon Choi**[6], **Lionel B. Ivashkiv**[2,4,7], **Hiroshi Takayanagi**[3], and **Ryutaro Kamijo**[1]

[1]Department of Biochemistry, School of Dentistry, Showa University, 1-5-8 Hatanodai, Shinagawa, Tokyo 142-8555, Japan

[2]Arthritis and Tissue Degeneration Program, Hospital for Special Surgery, New York, New York 10021, USA

[3]Department of Cell Signaling, Graduate School, Tokyo Medical and Dental University, Yushima 1-5-45, Bunkyo-ku, Tokyo 113-8549, Japan and Global Center of Excellence Program, International Research Center for Molecular Science in Tooth and Bone Diseases

[4]Department of Medicine, Weill Cornell Medical College, New York, New York 10021, USA

[5]Laboratory of Molecular Growth Regulation, National Institute of Child Health and Human Development, National Institutes of Health, Bethesda, Maryland 20892, USA

[6]Department of Pathology and Laboratory Medicine, University of Pennsylvania School of Medicine, Philadelphia, PA 19104, USA

[7]Graduate Program in Immunology and Microbial Pathogenesis, Weill Graduate School of Medical Sciences of Cornell University, New York, New York 10021, USA

Abstract

Bone metabolism results from a balance between osteoclast-driven bone resorption and osteoblast-mediated bone formation. Diseases such as periodontitis and rheumatoid arthritis are characterized by increased bone destruction due to enhanced osteoclastogenesis[1,2]. Here we report that interferon regulatory factor 8 (IRF8), a transcription factor expressed in immune cells, is a key regulatory molecule for osteoclastogenesis. IRF8 expression in osteoclast precursors was downregulated during the initial phase of osteoclast differentiation induced by receptor activator of nuclear factor κB ligand (RANKL, also called TRANCE, ODF, and OPGL), which is encoded by the *Tnfsf11* gene. Mice deficient in IRF8 exhibited severe osteoporosis due to increased numbers of osteoclasts, and enhanced bone destruction following lipopolysaccharide (LPS) administration. *Irf8*$^{-/-}$ osteoclast precursors underwent increased osteoclastogenesis in response to RANKL and tumor necrosis factor α (TNFα). IRF8 suppressed osteoclastogenesis by inhibiting the function and expression of nuclear factor of activated T cells c1 (NFATc1). Our results show that IRF8 inhibits osteoclast formation

Correspondence should be addressed to M.T. (takami@dent.showa-u.ac.jp).

AUTHOR CONTRIBUTIONS

B.Z. performed most of the experiments with significant assistance from M.T. X.W. conducted the histological analysis. A.Y., T.K., X.H., and T.T. assisted with the experiments. K.O. provided the *Irf8*$^{-/-}$ mice. B.Z. and M.T. designed the project and wrote the manuscript. Y.C. provided recombinant RANKL and contributed to manuscript preparation. L.B.I. oversaw the bone marrow chimera and human cell experiments and contributed to manuscript revision. H.T. oversaw the inflammatory bone destruction experiments and provided critical advice for the experiments. M.T. and R.K. supervised the project.

COMPETING INTERESTS STATEMENT

The authors declare that they have no competing financial interests.

under physiological and pathological conditions, and suggest a model where downregulation of inhibitory factors like IRF8 contributes to RANKL-mediated osteoclastogenesis.

Osteoclasts are multinucleated giant cells derived from the monocyte/macrophage lineage. Their differentiation is triggered by RANKL in the presence of macrophage colony-stimulating factor (M-CSF, encoded by *Csf-1* gene), which is produced by osteoblasts[1,2]. RANKL induces intracellular signals via its receptor RANK, and upregulates the expression of various genes, such as *Nfatc1*,*fos, Oscar, Ctsk*, and *Calcr* that encode proteins for NFATc1, c-Fos, OSCAR, cathepsin K and calcitonin receptor, respectively[3–5]. Numerous studies have focused on these upregulated genes and their roles in osteoclastogenesis. On the other hand, the expression levels of various genes are simultaneously downregulated during osteoclastogenesis[6]. The biological significance of the downregulated expression of these genes following RANK activation, however, has not been fully elucidated.

To identify genes that show reduced expression levels in response to RANK signaling, we performed a genome-wide screening of mRNAs from osteoclast precursors and osteoclasts using a DNA microarray technique (data not shown). Among the identified genes, expression of the transcription factor *Irf8* [also called interferon consensus sequence binding protein (ICSBP)] was found to be downregulated during the initial phase of osteoclastogenesis triggered by RANKL (data not shown). IRF8 is known to be specifically expressed in immune cells, including monocytes/macrophages, B lymphocytes, and activated T lymphocytes[7–9]. It is a member of the IRF family and has been shown to regulate myeloid cell development by interacting with the Ets family transcription factors[10,11]. Hence, *Irf8*$^{-/-}$ mice show an increased number of myeloid progenitors, defects in macrophage function including impaired IL-12 production, developmental defects in CD8α^{+} and plasmacytoid dendritic cells, and systemic expansion of the granulocyte population, which frequently leads to a fatal blast crisis[12–14].

Using RT-PCR and immunoblot analysis, IRF8 expression was detected in bone marrow-derived macrophages (BMMs) and spleen-derived macrophages, which are capable of differentiating into osteoclasts (Fig. 1a,b). As previously shown[3], NFATc1 was modestly expressed at a basal level in unstimulated BMMs and NFATc1 expression was strongly induced after RANKL stimulation (Fig. 1b); robust induction of NFATc1 by RANKL is a necessary and pivotal step for osteoclast differentiation characterized by enhanced expression of osteoclast marker genes such as *Oscar*, *Itgb3* that encodes integrin β3 protein, and *Ctsk*[3]. In contrast, IRF8 expression decreased after RANKL stimulation (Fig. 1a,b), resulting in substantially lower nuclear IRF8 protein 24 h after RANKL addition (Fig. 1b). We hypothesized that IRF8 downregulation may be required for osteoclast differentiation and that IRF8 may inhibit early stages of osteoclastogenesis.

To examine the role of IRF8 in osteoclastogenesis, we constructed a retroviral vector, *pMX-Irf8-IRES-EGFP*, which was engineered to express both IRF8 and enhanced green fluorescence protein (EGFP). Macrophage-like osteoclast precursors were transduced with retroviral particles encoding *Irf8* or control viral particles that lacked the *Irf8* sequence (pMX-IRES-*EGFP*). IRF8–overexpressing precursors failed to differentiate into osteoclasts in response to RANKL stimulation (Fig. 1c). Furthermore, these cells were able to phagocytize zymosan particles, whereas multinucleated osteoclasts failed to do so (Fig. 1d). These results suggest that IRF8 inhibits osteoclastogenesis from precursor cells, which instead retain the characteristics of phagocytic macrophages.

Next, we analyzed the *Irf8*$^{-/-}$ mice for abnormal bone phenotypes. Radiographic and microcomputed tomographic analyses showed that these mice had severe osteoporosis accompanied by dramatic decreases in trabecular bone volume, number, and thickness, as well as the number of bone nodules (Fig. 2a, b). Histomorphometric analysis also revealed reduced

bone mass in the *Irf8*$^{-/-}$ mice (data not shown). Importantly, increases in the osteoclast number and surface area were observed in these mice (Fig. 2c). There were no significant differences between wild-type and *Irf8*$^{-/-}$ mice in the serum level of osteoprotegerin (OPG encoded by *Tnfrsf11b* gene), a decoy RANKL receptor that inhibits osteoclastogenesis, or in RANKL levels in primary cultured osteoblasts (Supplementary Fig. 1 online). Moreover, an increased rate of bone formation accompanying the accelerated bone resorption rate was observed in the *Irf8*$^{-/-}$ mice, suggesting that their osteoporosis was caused by enhanced bone turnover and remodeling (Fig. 2d). Together, these observations indicated that IRF8 plays a suppressive role in osteoclastogenesis during *in vivo* bone remodeling. To address whether the bone phenotype could be explained by *Irf8* deficiency in osteoclast precursors, or whether a cell autonomous effect of *Irf8* deficiency in osteoblasts or bone marrow stromal cells could play a role, we established chimeric mouse models in which either wild-type or *Irf8*$^{-/-}$ littermate bone marrow was transplanted into lethally irradiated wild-type recipients. Consistent with the global *Irf8* deficient mice, *Irf8*$^{-/-}$ bone marrow chimeric mice showed severe high turnover osteoporosis (Fig. 2e–h). IRF8 is mainly expressed in hematopoietic cells[7–9]. Indeed, IRF8 expression was not detected in primary calvarial osteoblasts (data not shown). Furthermore, primary *Irf8*$^{-/-}$ osteoblast differentiation and matrix calcification were not affected compared to wild-type cells (Supplementary Fig. 2 online). Thus, the osteoporosis resulted from enhanced osteoclastogenesis, which is a cell autonomous consequence of *Irf8* deficiency in osteoclast precursors but not osteoblasts.

On the basis of these results, we examined the differentiation potential of osteoclast precursors obtained from *Irf8*$^{-/-}$ mice. When wild-type or *Irf8*$^{-/-}$ osteoclast precursors were cocultured with wild-type or *Irf8*$^{-/-}$ primary osteoblasts in the presence of active vitamin D_3 (an inducer of RANKL expression in osteoblasts), a greater number of osteoclasts formed from the *Irf8*$^{-/-}$ precursors than from the wild-type cells, independent of whether the osteoblasts were from *Irf8*$^{-/-}$ or wild-type mice (Fig. 3a). These data further support the notion that there is no difference in osteoclastogenic activity between wild-type and *Irf8*$^{-/-}$ osteoblasts, and that *Irf8* deficiency in osteoclast precursors plays a decisive role in promoting osteoclast differentiation. Indeed, macrophage cultures prepared from *Irf8*$^{-/-}$ mice also exhibited augmented osteoclastogenesis in the presence of RANKL and M-CSF (Fig. 3b), which led to an increase in resorption on dentin slices *in vitro* (data not shown). On the other hand, retrovirus-mediated reconstitution of IRF8 expression in *Irf8*$^{-/-}$ macrophages inhibited RANKL-induced osteoclastogenesis (Fig. 3c). These results demonstrate that IRF8 in osteoclast precursors is involved in the inhibition of osteoclastogenesis *in vitro* and *in vivo*. Furthermore, we found that IRF8 expression was also decreased during RANKL-induced human osteoclastogenesis, although with slower kinetics (Fig. 3d). Silencing of *Irf8* mRNA in human osteoclast precursors by siRNAs resulted in enhanced osteoclast differentiation (Fig. 3e–f), indicating the function of IRF8 in osteoclastogenesis is well conserved in humans and mice.

Consistent with the results regarding osteoclastogenesis, the mRNA expression profiles of various osteoclast markers were more strongly upregulated by RANKL stimulation in macrophages prepared from *Irf8*$^{-/-}$ mice compared with those obtained from wild-type mice (Supplementary Fig. 3 online). However, *Rank* and *c-fms* mRNA expression and RANK cell surface protein expression were comparable in wild-type and *Irf8*$^{-/-}$ osteoclast precursors (Supplementary Fig. 4a online and data not shown). During osteoclast precursor generation from bone marrow cells, M-CSF treatment did not lead to a greater increase in *Rank* mRNA expression in *Irf8*$^{-/-}$ cells than in control cells (Supplementary Fig. 4b online). These results suggest that enhanced osteoclastogenesis in *Irf8*$^{-/-}$ macrophages is not due to changes in these receptor levels.

Expression of *Nfatc1* gene and the osteoclast marker *Acp5* gene that encodes tartrate-resistant acid phosphatase (TRAP) protein in *Irf8*$^{-/-}$ precursors was induced by concentrations of RANKL that were 5%–25% of those required for the expression of these genes in wild-type precursors (Fig. 4a). Furthermore, overexpression of IRF8 in the precursor cells repressed the RANKL-induced expression of *Nfatc1* and *Acp5* mRNAs (Fig. 4b).

These observations led us to examine the effect of IRF8 on the transcriptional activity of NFATc1, which was previously reported to interact with IRF8[15]. For these experiments, we employed luciferase reporter plasmids driven by three copies of the NFATc1 binding site from the human *IL-2* distal promoter (p3x *Nfatc1-Luc*) or by the mouse *Acp5* promoter (p*Acp5-Luc*). Overexpression of *Nfatc1* gene activated these promoters, whereas simultaneous expression of *Irf8* gene reduced the activities of the promoters to control levels (Fig. 4c), indicating that IRF8 inhibits the transcriptional activity of NFATc1. When GST-IRF8 proteins were incubated with nuclear lysates containing FLAG-hemagglutinin-tagged NFATc1 (FH-NFATc1), anti-FLAG antibodies resulted in the coimmunoprecipitation of GST-IRF8 and FH-NFATc1, suggesting that IRF8 physically interacts with NFATc1 (Fig. 4d). Furthermore, association of endogenous IRF8 and NFATc1 was identified by co-immunoprecipitation from nuclear extracts of human monocytic cells (Supplementary Fig. 5 online). We further examined the effects of IRF8 on the binding of NFATc1 to its target DNA elements in an electrophoretic mobility shift assay (EMSA); NFATc1-DNA complexes were detected, which was confirmed by the addition of competitive probes or anti-NFATc1 antibodies. Increased levels of GST-IRF8 or nuclear lysates containing excess IRF8, however, significantly decreased the binding of NFATc1 to the probes (Fig. 4e, f), demonstrating the inhibitory effect of IRF8 on NFATc1 binding to its target DNA elements.

We then attempted to examine the roles of IRF8 in the processes underlying pathological bone destruction. Because several members of the IRF family of transcription factors, including IRF8, have been demonstrated to play crucial roles in toll-like receptor (TLR) signaling in response to such microbial components as LPS and unmethylated CpG DNA[16,17], we examined the role of IRF8 in the bone destruction observed during TLR-mediated inflammation. Administration of LPS to the calvarial periosteum resulted in enhanced osteoclast formation in wild-type mice, whereas more extensive bone destruction was observed in *Irf8*$^{-/-}$ mice (Fig. 4g). These results suggest that IRF8 is a critical negative regulator of osteoclastogenesis and a mediator of the maintenance of bone integrity during inflammatory bone destruction. We also examined the effects of TLR ligands on osteoclastogenesis in wild-type and *Irf8*$^{-/-}$ osteoclast precursors. As previously reported[18], LPS at high doses completely inhibited RANKL-induced osteoclastogenesis in wild-type cell cultures. In contrast, corresponding high doses of LPS, and also of the TLR3 ligand poly(I:C) and the TLR9 ligand CpG DNA, only partially inhibited osteoclast differentiation in *Irf8*$^{-/-}$ cell cultures (Fig. 4h and Supplementary Fig. 6 on line). *Irf8*-deficient cells were almost completely refractory to the inhibitory effects of the TLR2 ligand peptidoglycan (Supplementary Fig. 6a). These results suggest a potential inhibitory role of IRF8 in the regulation of osteoclastogenesis by TLRs, although TLRs can also activate IRF8-independent inhibitory mechanisms. We further found that *Ifnα/β* expression was not diminished in *Irf8*-deficient cells, and that IFN-γ completely inhibited osteoclastogenesis in *Irf8*$^{-/-}$ macrophages, similar to wild-type cells (data not shown), thus suggesting that IRF8 can inhibit osteoclastogenesis independently of IFN-γ.

Finally, we examined the effect of TNFα on osteoclastogenesis using *Irf8*$^{-/-}$ precursors, because TNFα is a critical mediator of inflammation induced by TLRs[19–21] and has been suggested to be able to induce osteoclastogenesis[22–24]. Consistent with previous reports, TNFα induced the development of a small number of osteoclasts in cultures of wild-type precursor cells (Fig. 4i). Notably, osteoclastogenesis was enhanced in cultures of *Irf8*$^{-/-}$ precursor cells treated with TNFα (Fig. 4i). The mRNA expression levels of *Nfatc1* and

Acp5 in the *Irf8*$^{-/-}$ osteoclast precursors were also augmented by TNFα (Fig. 4j), indicating that IRF8 also plays a suppressive role in TNFα–induced osteoclastogenesis.

Our data provide a mechanism by which IRF8 suppresses osteoclastogenesis (depicted in Supplementary Fig. 7 on line). In osteoclast precursors, abundant IRF8 interacts with basally expressed NFATc1 to suppress its transcriptional activity and thus prevent its activation of target genes, including autoamplification of its own promoter. Stimulation of osteoclast precursors with RANKL results in the activation of NF-κB and AP-1 that bind to the *Nfatc1* promoter to induce its activity. At the same time, RANKL induces the downregulation of IRF8, thereby releasing NFATc1 from IRF8-mediated suppression and augmenting NFATc1-mediated auto-amplification of its own expression. Together, these mechanisms result in robust NFATc1 expression and induction of downstream genes required for osteoclast differentiation.

Bone erosion that occurs in the setting of infection and chronic inflammation, termed inflammatory osteolysis, contributes to the pathogenesis of infectious and inflammatory diseases such as rheumatoid arthritis[25]. Inflammatory bone erosion is driven by microbial products such as LPS and inflammatory cytokines including TNFα that activate osteoclastogenesis directly or indirectly via activation of stromal cells and osteoblasts[25]. Our findings show that IRF8 plays an important role in attenuating LPS-induced inflammatory bone resorption and LPS- and TNFα-induced osteoclastogenesis. This homeostatic role of IRF8 may be important during acute infections and also in chronic inflammatory conditions such as rheumatoid arthritis. Identification of additional factors and mechanisms that augment IRF8 expression or function may represent a fruitful approach to therapeutic suppression of inflammatory bone erosion.

Overall, our findings support a model of RANKL-induced NFATc1 expression and osteoclast differentiation that involves cooperation between RANKL-mediated induction of positive regulators of osteoclastogenesis and suppression of negative regulators of osteoclast differentiation such as IRF8.

Methods

Mice and analysis of bone phenotypes

The *Irf8*$^{-/-}$ mice (C57BL/6) used in this study have been described previously[12]. Tetracycline hydrochloride (20 mg/kg; Sigma) and, 72 h later, calcein (10 mg/kg; Wako) were injected subcutaneously into 8-week-old wild-type and *Irf8*$^{-/-}$ mice. The mice were then euthanized 32 h after the second injection. The LPS-induced model of bone loss has been described previously[26], except that 12.5 mg/kg LPS (Sigma) was used in the present study. The mice were subjected to histomorphometric and microradiographic examinations as described previously[27]. All mice were born and maintained under specific pathogen-free conditions. All animal experiments were approved by and conducted according to the guidelines of the Showa University Animal Care and Use Committee (approval number: 17079).

Generation of bone marrow chimeric mice

Donor bone marrow cells from wild-type or *Irf8*$^{-/-}$ littermate mice (on C57/BL6 background) were harvested and one-fourth of total bone marrow cells from each donor were injected intravenously via tail vein into each of the irradiated wild-type recipients. Recipient mice (3-week-old C57/BL6 mice) were obtained from Jackson Laboratory and were lethally irradiated with a single dose of 875 rads 1 day prior to transplantation. Chimeric mice were sacrificed 8 weeks after bone marrow transplantation. The experiments using chimeric mice were approved by the Hospital for Special Surgery Institutional Animal Care and Use Committee.

In vitro assays of osteoclast differentiation and macrophage function

The method used to analyze osteoclast differentiation *in vitro* has been described previously[28]. Briefly, mouse bone marrow or spleen cells were cultured with 50 ng/ml M-CSF for 3 days. The obtained BMMs or spleen-derived macrophages were further stimulated with 150 ng/ml RANKL in the presence of 50 ng/ml M-CSF for 3–4 days. We also cocultured bone marrow cells, BMMs, or spleen-derived macrophages with primary osteoblasts derived from mouse calvaria in the presence of 10^8 M 1,25 $(OH)_2D_3$ and 10^{-6} M prostaglandin E_2 for 6 days. Media were changed every 2 days. Generation of osteoclasts was evaluated by TRAP staining and its activity assays[28]. Methods used for the phagocytosis assay and labeling of actin have been described previously[28].

Human osteoclast culture system and RNAi

Human fresh peripheral blood mononuclear cells (PBMCs) were obtained from whole blood from disease-free volunteers. Human $CD14^+$ monocytes were then purified from PBMCs with anti-CD14 magnetic beads (Miltenyi Biotec) and were cultured in α-MEM medium with 10% FBS (Hyclone) and 20 ng/ml of M-CSF (Peprotech) for 2 days to induce osteoclast precursors that were further stimulated with RANKL in the presence of 20 ng/ml of M-CSF for 3–6 days to generate human osteoclasts. The experiments using human cells were approved by the Hospital for Special Surgery Institutional Review Board. Short interfering RNAs (siRNAs) specifically targeting human *Irf8* or control siRNAs (Dharmacon, Invitrogen) were transfected into primary human $CD14^+$ monocytes with the Amaxa Nucleofector device set to program Y-001 using the Human Monocyte Nucleofector kit (Amaxa). Two different targeting siRNAs and control siRNAs were used with comparable results in a total of 6 independent experiments with different blood donors.

Plasmid constructs

Irf8 cDNA was prepared and amplified in RT-PCRs using RNA from BMMs. The coding region of *Irf8* was PCR-amplified using the following primers: 5'-GCAGGATGTGTGACCGGAAC-3' (sense) and 5'-ACTGAGGCTTAGACGGTGAT-3' (antisense). The amplified PCR fragment was subcloned into a pCR-Blunt vector to produce pCR-Blunt-*Irf8* using a Zero Blunt PCR Cloning kit (Invitrogen). The *pMX-Irf8-IRES-EGFP* retroviral vector was constructed by inserting a 1.3-kb EcoRI/EcoRI DNA fragment encoding *Irf8* from pCR-Blunt-*Irf8* into the same site in the pMX-IRES-*EGFP* vector. The 1.3-kb BamHI/XhoI DNA fragment encoding IRF8 from *pMX-Irf8-IRES-EGFP* was then inserted into the same site in the *pMX-puro* vector to construct the *pMX-Irf8-puro* retroviral vector. The pcDNA3-*Irf8* expression vector was constructed by inserting a 1.3-kb BamHI/NotI DNA fragment encoding IRF8 from *pMX-Irf8-IRES-EGFP* into the same site in the pcDNA3 vector. pcDNA3-*Nfatc1* was constructed by inserting an EcoRI/EcoRI DNA fragment encoding NFATc1 from *pMX-Nfatc1-IRES-EGFP* 3 into the same site in the pcDNA3 vector. The *pFH-Nfatc1*, *p3×Nfatc-Luc*, and *pAcp5-Luc* vectors were previously described[3,29].

Statistical analysis

Statistical analysis was performed using Student *t*-tests ($p < 0.05$ was taken as statistically significant) and all data are presented as the mean ± s.e.m. Results are representative of more than four individual experiments.

Additional methods

Details of the methods including retroviral gene transduction, GeneChip, RT-PCR, Northern blot assay, Real-time PCR, Luciferase reporter assay, preparation of GST fusion proteins,

immunoprecipitation and immunoblot analyses, and EMSA are described in Supplementary Methods on line.

Supplementary Material

Refer to Web version on PubMed Central for supplementary material.

ACKNOWLEDGMENTS

We are grateful to Dr. M. Asagiri (Tokyo Medical and Dental University) for great technical assistance. We thank Dr. T. Kitamura (University of Tokyo) for providing the retrovirus expression system. We also thank Dr. A. Mochizuki and all members of the Department of Biochemistry, School of Dentistry, Showa University for valuable discussion. This work is supported in part by High-Tech Research Center Project for Private Universities from the Ministry of Education, Culture, Sports, Science and Technology, Japan, 2005–2009, and by Grants-in-Aid for Scientific Research from the Japan Society for the Promotion of Science (20390474 to M.T.), and by grants from the NIH (AR053843 and DE19381 to Y.C., and DE019420 and AR46713 to L.B.I.).

REFERENCES

1. Wada T, Nakashima T, Hiroshi N, Penninger JM. RANKL-RANK signaling in osteoclastogenesis and bone disease. Trends Mol Med 2006;12:17–25. [PubMed: 16356770]
2. Lee SK, Lorenzo J. Cytokines regulating osteoclast formation and function. Curr Opin Rheumatol 2006;18:411–418. [PubMed: 16763463]
3. Takayanagi H, et al. Induction and activation of the transcription factor NFATc1 (NFAT2) integrate RANKL signaling in terminal differentiation of osteoclasts. Dev Cell 2002;3:889–901. [PubMed: 12479813]
4. Grigoriadis AE, et al. c-Fos: a key regulator of osteoclast-macrophage lineage determination and bone remodeling. Science 1994;266:443–448. [PubMed: 7939685]
5. Kim N, Takami M, Rho J, Josien R, Choi Y. A novel member of the leukocyte receptor complex regulates osteoclast differentiation. J Exp Med 2002;195:201–219. [PubMed: 11805147]
6. Ishida N, et al. Large scale gene expression analysis of osteoclastogenesis in vitro and elucidation of NFAT2 as a key regulator. J Biol Chem 2002;277:41147–41156. [PubMed: 12171919]
7. Kantakamalakul W, et al. Regulation of IFN consensus sequence binding protein expression in murine macrophages. J Immunol 1999;162:7417–7425. [PubMed: 10358195]
8. Nelson N, et al. Expression of IFN regulatory factor family proteins in lymphocytes. Induction of Stat-1 and IFN consensus sequence binding protein expression by T cell activation. J Immunol 1996;156:3711–3720. [PubMed: 8621906]
9. Driggers PH, et al. An interferon gamma-regulated protein that binds the interferon-inducible enhancer element of major histocompatibility complex class I genes. Proc Natl Acad Sci U S A 1990;87:3743–3747. [PubMed: 2111015]
10. Tamura T, Ozato K. ICSBP/IRF-8: its regulatory roles in the development of myeloid cells. J Interferon Cytokine Res 2002;22:145–152. [PubMed: 11846985]
11. Marecki S, Fenton MJ. PU.1/Interferon Regulatory Factor interactions: mechanisms of transcriptional regulation. Cell Biochem Biophys 2000;33:127–148. [PubMed: 11325034]
12. Holtschke T, et al. Immunodeficiency and chronic myelogenous leukemia-like syndrome in mice with a targeted mutation of the ICSBP gene. Cell 1996;87:307–317. [PubMed: 8861914]
13. Tamura T, Nagamura-Inoue T, Shmeltzer Z, Kuwata T, Ozato K. ICSBP directs bipotential myeloid progenitor cells to differentiate into mature macrophages. Immunity 2000;13:155–165. [PubMed: 10981959]
14. Schiavoni G, et al. ICSBP is essential for the development of mouse type I interferon-producing cells and for the generation and activation of CD8alpha(+) dendritic cells. J Exp Med 2002;196:1415–1425. [PubMed: 12461077]
15. Zhu C, et al. Activation of the murine interleukin-12 p40 promoter by functional interactions between NFAT and ICSBP. J Biol Chem 2003;278:39372–39382. [PubMed: 12876285]

16. Tsujimura H, et al. Toll-like receptor 9 signaling activates NF-kappaB through IFN regulatory factor-8/IFN consensus sequence binding protein in dendritic cells. J Immunol 2004;172:6820–6827. [PubMed: 15153500]
17. Zhao J, et al. IRF-8/interferon (IFN) consensus sequence-binding protein is involved in Toll-like receptor (TLR) signaling and contributes to the cross-talk between TLR and IFN-gamma signaling pathways. J Biol Chem 2006;281:10073–10080. [PubMed: 16484229]
18. Takami M, Kim N, Rho J, Choi Y. Stimulation by toll-like receptors inhibits osteoclast differentiation. J Immunol 2002;169:1516–1523. [PubMed: 12133979]
19. O'Neill LA. How Toll-like receptors signal: what we know and what we don't know. Curr Opin Immunol 2006;18:3–9. [PubMed: 16343886]
20. Akira S, Uematsu S, Takeuchi O. Pathogen recognition and innate immunity. Cell 2006;124:783–801. [PubMed: 16497588]
21. Takaoka A, et al. Integral role of IRF-5 in the gene induction programme activated by Toll-like receptors. Nature 2005;434:243–249. [PubMed: 15665823]
22. Azuma Y, Kaji K, Katogi R, Takeshita S, Kudo A. Tumor necrosis factor-alpha induces differentiation of and bone resorption by osteoclasts. J Biol Chem 2000;275:4858–4864. [PubMed: 10671521]
23. Kobayashi K, et al. Tumor necrosis factor alpha stimulates osteoclast differentiation by a mechanism independent of the ODF/RANKL-RANK interaction. J Exp Med 2000;191:275–286. [PubMed: 10637272]
24. Kim N, et al. Osteoclast differentiation independent of the TRANCE-RANK-TRAF6 axis. J Exp Med 2005;202:589–595. [PubMed: 16147974]
25. Lorenzo J, Horowitz M, Choi Y. Osteoimmunology: interactions of the bone and immune system. Endocr Rev 2008;29:403–440. [PubMed: 18451259]
26. Takayanagi H, et al. T-cell-mediated regulation of osteoclastogenesis by signalling cross-talk between RANKL and IFN-gamma. Nature 2000;408:600–605. [PubMed: 11117749]
27. Takayanagi H, et al. RANKL maintains bone homeostasis through c-Fos-dependent induction of interferon-beta. Nature 2002;416:744–749. [PubMed: 11961557]
28. Mochizuki A, et al. Identification and characterization of the precursors committed to osteoclasts induced by TNF-related activation-induced cytokine/receptor activator of NF-kappa B ligand. J Immunol 2006;177:4360–4368. [PubMed: 16982870]
29. Koga T, et al. NFAT and Osterix cooperatively regulate bone formation. Nat Med 2005;11:880–885. [PubMed: 16041384]

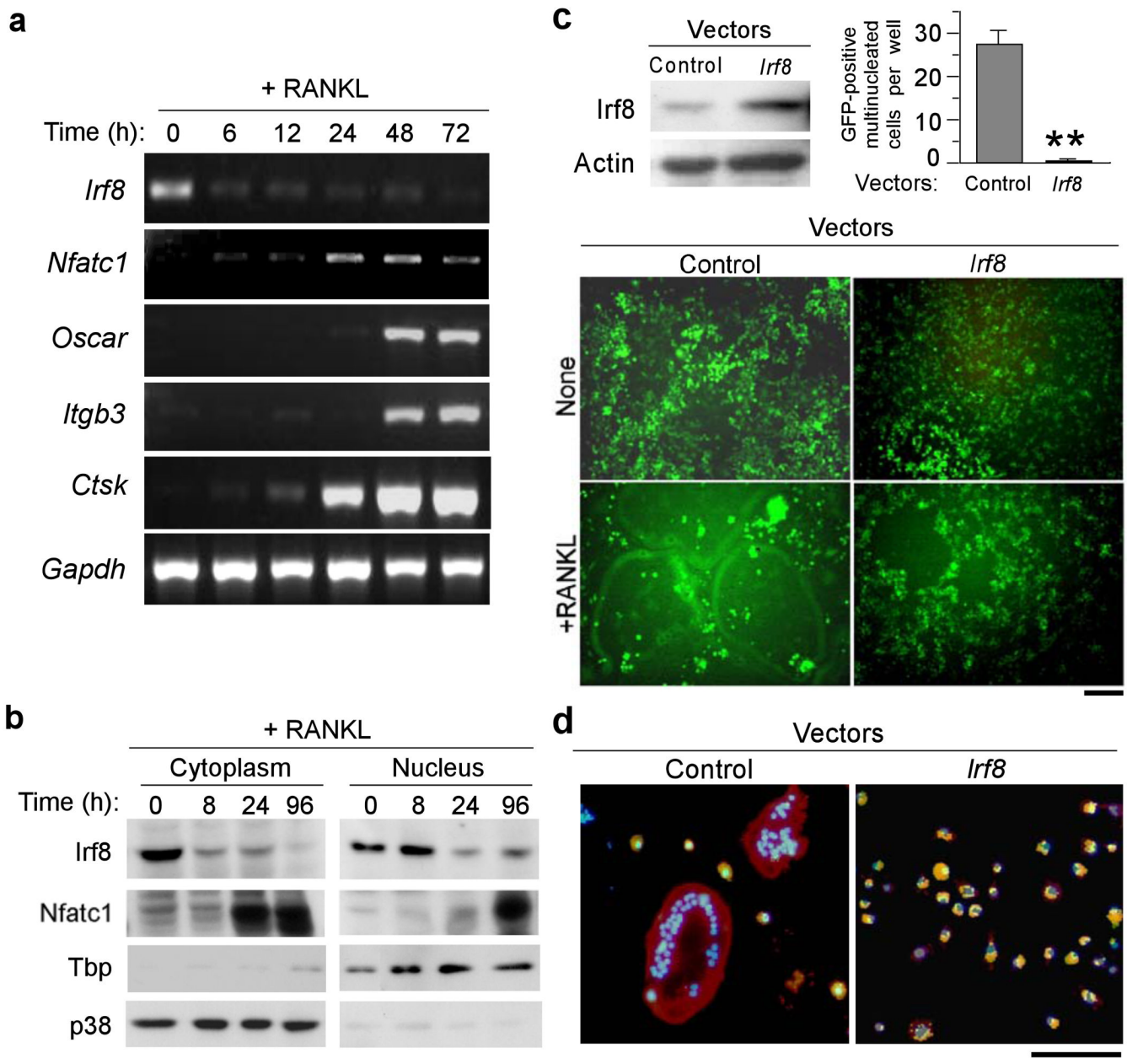

Figure 1.

IRF8 inhibits osteoclastogenesis in BMMs stimulated with M-CSF and RANKL. (**a**) mRNA expressions of *Irf8*, *Nfatc1*, *Oscar*, *Itgb3*, *Ctsk* and *Gapdh* in BMMs 0, 6, 12, 24, 48 and 72 h after M-CSF (50 ng/ml) and RANKL (150 ng/ml) stimulation (RT-PCR). (**b**) Immunoblot analysis of IRF8 and NFATc1 expressions in cytoplasmic and nuclear fractions of BMMs obtained 0, 8, 24 and 96 h after stimulation with M-CSF and RANKL. Expression levels of TBP and p38 were measured as loading controls for nuclear and cytoplasmic fractions, respectively. (**c**) Inhibition of GFP-positive multinucleated cell (osteoclast) formation due to retrovirus-mediated overexpression of IRF8 in BMMs. Overexpression of IRF8 protein in BMMs was confirmed by immunoblotting (top left). GFP-positive multinucleated cells were counted (top right). GFP-positive multinucleated cells appear green giant cells (bottom). Control, *pMX-IRES-EGFP*; Irf8, pMX-*Irf8-IRES-EGFP*. ***P*<0.01. Bar, 50 μm. (**d**) BMMs

were transduced with pMX-*puro* (control) or pMX-*Irf8-puro (Irf8)* and stimulated with M-CSF and RANKL for 3 days. Phagocytic activity was examined using FITC-conjugated zymosan bioparticles (green). F-actin was labeled with rhodamine-conjugated phalloidin (red). Nuclei were stained with DAPI (blue). Colocalization of zymosan and actin is denoted by the yellow fluorescent signals. Bar, 100 μm.

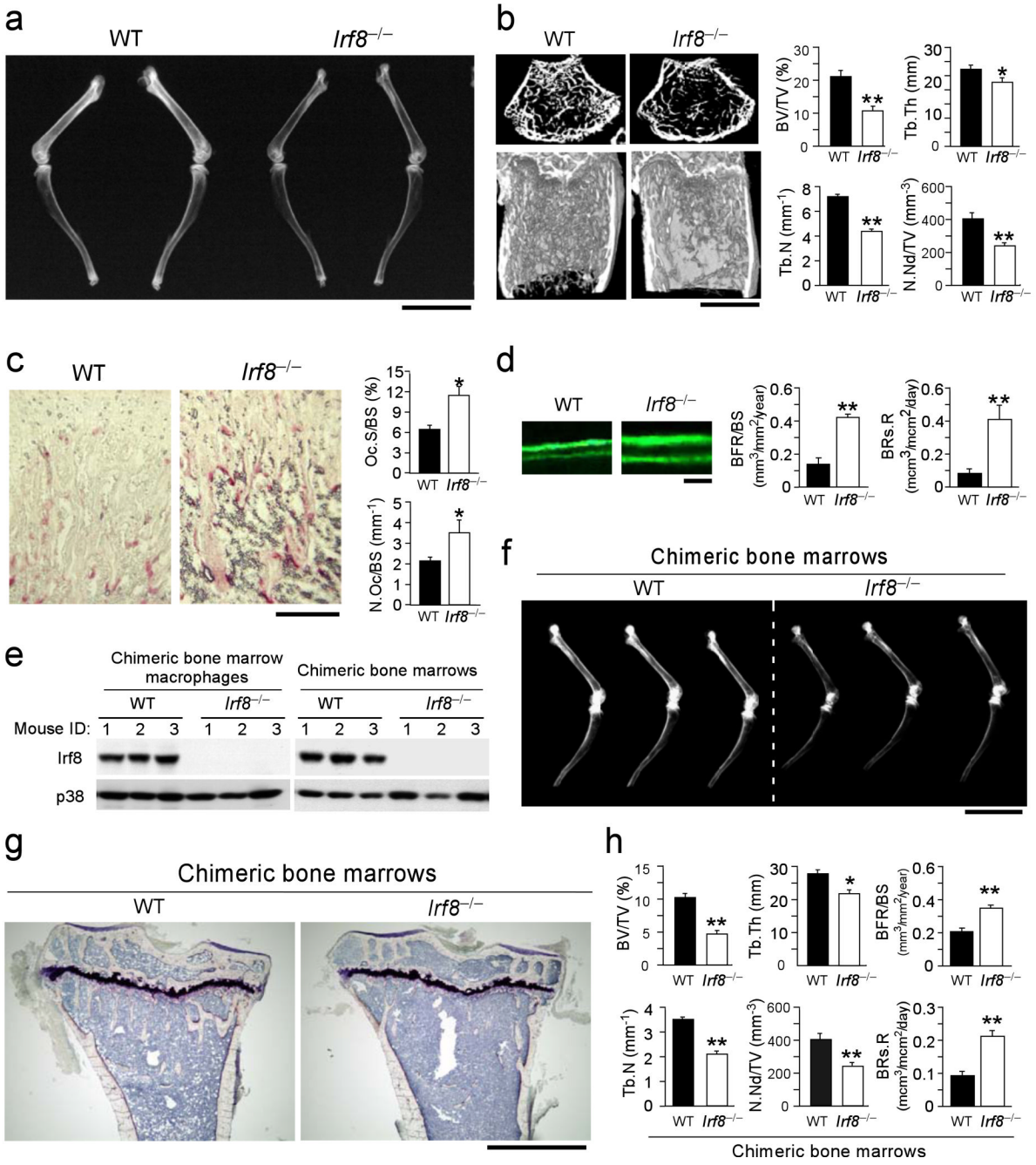

Figure 2.

Irf8$^{-/-}$ mice exhibit severe osteoporosis due to enhanced osteoclast formation. (**a**) Radiographic analysis of the femur and tibia. Bar, 1 cm. (**b**) Microcomputed tomography of the femurs of 8-week-old wild-type and *Irf8*$^{-/-}$ mice (left), and bone morphometric analysis of femurs isolated from8-week-old mice (n = 6 in each group) (right). BV/TV, bone volume per tissue volume; Tb.Th, trabecular bone thickness; Tb.N, trabecular number; N.Nd/TV, number of nodules per tissue volume. ***P*<0.01; **P*<0.05. Bar, 500 μm (**c**) Histology of femurs from 8-week-old mice in which osteoclasts were stained using TRAP, an enzymatic marker of osteoclasts (left), and histomorphometric analysis of tibias from 8-week-old mice (n=5 in each group) (right). Oc.S/BS, osteoclast surface per bone surface; N.Oc/BS, number of osteoclasts

per bone surface. **P*<0.05. Bar, 100 μm. (**d**) Histological photographs of bone formation that show tetracycline-calcein double labeling, which were administered with an interval of 72 h (left), and histomorphometric analysis of the bone formation rate and bone resorption rate in 8-week-old mice (right). BFR/BS, bone formation rate per bone surface; BRs.R, bone resorption rate. ***P*<0.01. (e) Analysis of IRF8 protein levels in BMs or M-CSF induced BMMs from recipient chimeric mice. (f) Soft-X ray photographs of long bones (tibias and femurs) isolated from chimeric mice. (g) Histological analysis of tibias isolated from chimeric mice (Villanueva bone staining). Bar, 500 μm. (h) Bone morphometric analysis of femurs isolated from chimeric mice. Representative data from one of two independent experiments is shown [n=3 (WT) and 3 (*Irf8*$^{-/-}$) in each experiment]. Data are expressed as the mean+SD (n=3). ***P*<0.01; **P*<0.05.

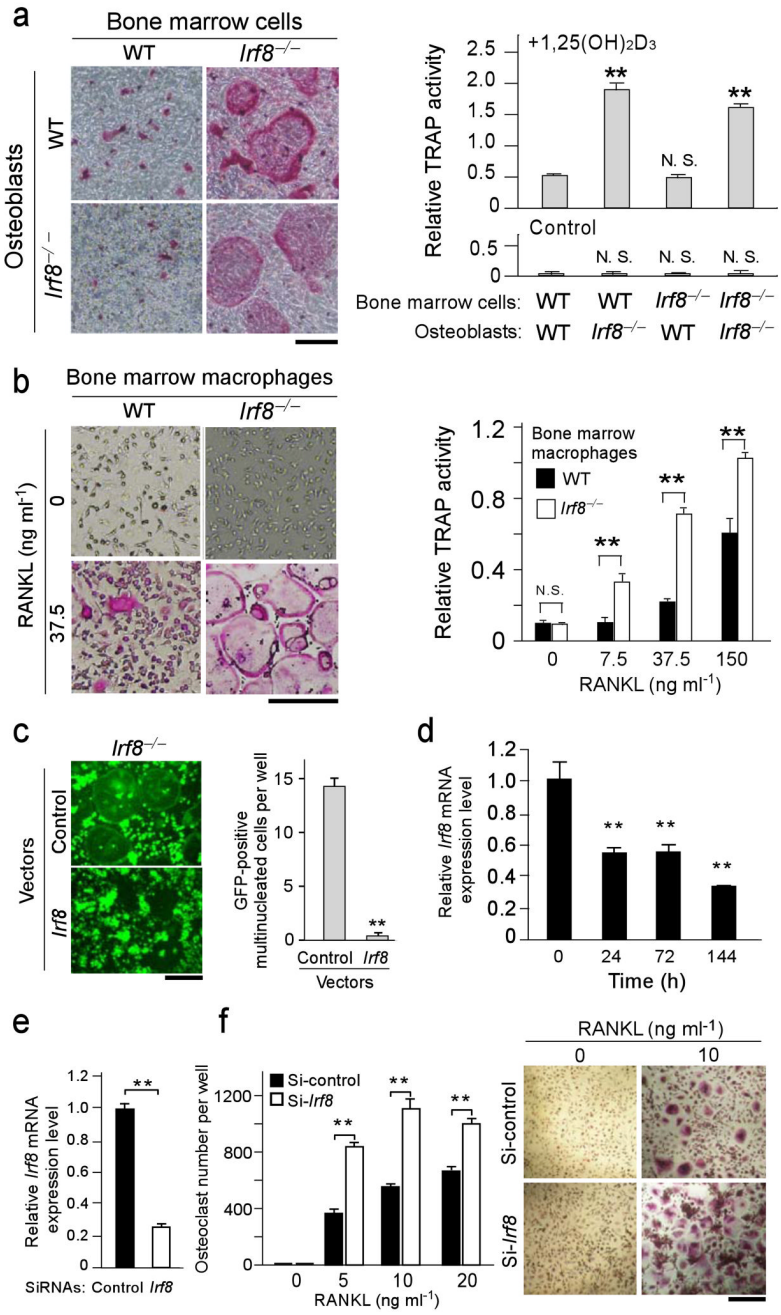

Figure 3.

IRF8 deficiency or RNAi-mediated silencing in osteoclast precursors leads to enhanced osteoclast formation. (**a**) Primary calvarial osteoblasts and bone marrow cells obtained from wild-type and *Irf8*$^{-/-}$ mice were cocultured in the presence of 10^{8} M $1,25(OH)_2D_3$ and 10^{-6} M prostaglandin E_2 (inducers of RANKL expression in osteoblasts) for 6 days. TRAP staining (left) and TRAP activity (right) of cultures are shown. Bar, 50 μm. (**b**) Osteoclast formation induced by 50 ng/ml M-CSF and the indicated doses of RANKL in BMM cultures. TRAP staining (left) and TRAP activity (right) of cultures are shown. Bar, 50 μm. (**c**) *Irf8*$^{-/-}$ macrophages were transduced with the vectors such as pMX-*Irf8*-IRES-*EGFP (Irf8)* or pMX-IRES-*EGFP* (Control) and stimulated with 150 ng/ml RANKL for 3 days (left). GFP-positive

multinucleated cells were counted as osteoclasts (right). ***P*<0.01. Bar, 50 μm. (**d**) Kinetics of *Irf8* mRNA expression during human osteoclastogenesis induced by 40 ng/ml RANKL at indicated time points. (**e**) Human CD14-positive monocytic cells were transfected with human *Irf8*-specific short interfering RNAs (si-*hIrf8*) or non-targeting control siRNAs (si-control), cultured for 2 days in the presence of 20 ng/ml M-CSF, and efficiency of silencing of *Irf8* mRNA was examined by quantitative real time-PCR. (**f**) The cells were further stimulated with indicated concentrations of RANKL for 6 days. Number of TRAP-positive multinucleated cells was counted as osteoclasts (left). TRAP-positive cells appear red in the photograph (right). ***P<0.01*. Representative data from one of three donors is shown; similar results were obtained using a distinct *Irf8*-specific siRNA in an additional three experiments. Data are expressed as the mean+SD of quad-duplicate cultures. ***P*<0.01; n.s., no statistical difference. Bar, 50 μm.

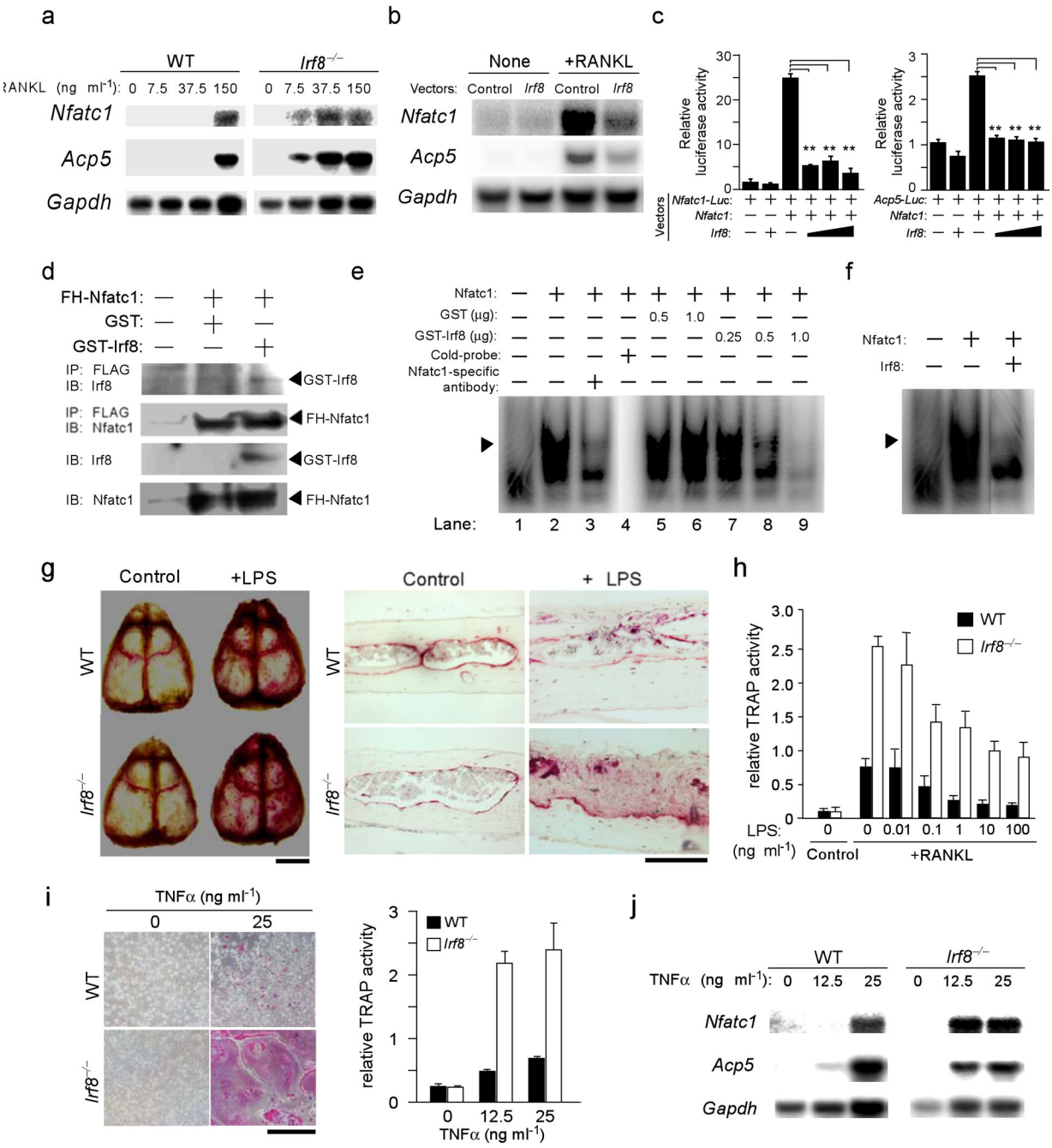

Figure 4.

IRF8 inhibits NFATc1 transcriptional activity and expression, and reduced IRF8 expression may contribute to pathological bone destruction. (**a**) Expression of *Nfatc1* and *Acp5* mRNAs induced by 24 h stimulation of BMMs derived from wild-type and *Irf8*$^{-/-}$ mice with 50 ng/ml M-CSF and the indicated doses of RANKL (Northern blotting). (**b**) Expression of *Nfatc1* and *Acp5* mRNAs in retrovirus-infected BMMs (Control, pMX-*puro; Irf8*, pMX-*Irf8-puro*) in the absence or presence of 150 ng/ml RANKL with 50 ng/ml M-CSF for 24 h (Northern blotting). *Gapdh* was used as an internal control. (**c**) A luciferase activity assay to examine the effect of IRF8 on the transcriptional activity of NFATc1. ***P*<0.01. (**d**) The interaction between NFATc1 and IRF8. IP, immunoprecipitation; IB, immunoblotting. (**e,f**) Analysis of the

inhibition of NFATc1 binding to its target DNA sequences using EMSAs (see supplementary methods on line). The arrow heads indicate a specific binding complex, which included the NFATc1–DNA complex; this was confirmed in a supershift assay (lane 1–3) and a cold competition experiment (lane 4). The intensity of NFATc1–DNA bands decreased with increasing amounts of GST-IRF8 (lanes 7–9), or when nuclear extracts from HEK293 cells cotransfected with *pcDNA3-Nfatc1* and pcDNA3-*Irf8* were used (**f**), but not with GST alone (lanes 5–6). (**g**) TRAP staining of mouse whole calvaria (left) and histological sections (right) obtained from wild-type and $Irf8^{-/-}$ mice with or without administration of LPS. (**h**) Osteoclast formation in BMMs stimulated with various doses of LPS in the presence of M-CSF (50 ng/ml) and RANKL (150 ng/ml) for 5 days. Data are expressed as the mean+SD of 4 cultures. (**i**) Left, BMM cultures in the presence of 50 ng/ml M-CSF and 0 or 25 ng/ml TNFα on day 3 shown by TRAP staining. Right, TNFα dose-dependent induction of osteoclast formation examined using TRAP activity assays. (**j**) Expression of *Nfatc1* and *Acp5* mRNAs in BMMs derived from wild-type and $Irf8^{-/-}$ mice stimulated with 50 ng/ml M-CSF and the indicated doses of TNFα for 24 h (Northern blotting).